JOURNAL OF THE AMERICAN COLLEGE OF CARDIOLOGY
© 2016 BY THE AMERICAN COLLEGE OF CARDIOLOGY FOUNDATION
PUBLISHED BY ELSEVIER

VOL. 67, NO. 3, 2016
ISSN 0735-1097/$36.00
http://dx.doi.org/10.1016/j.jacc.2015.10.092

Myocardial Infarction Alters Adaptation of the Tethered Mitral Valve

Jacob P. Dal-Bianco, MD,*‡ Elena Aikawa, MD, PhD,‡§ Joyce Bischoff, PhD,‡‖¶ J. Luis Guerrero, BS,† Jesper Hjortnaes, MD,§ Jonathan Beaudoin, MD,*‡ Catherine Szymanski, MD,*‡ Philipp E. Bartko, MD, PhD,* Margo M. Seybolt, BS,† Mark D. Handschumacher, BS,* Suzanne Sullivan, BS,† Michael L. Garcia, MA,† Adam Mauskapf, BA,† James S. Titus, BS,† Jill Wylie-Sears, MS,‖ Whitney S. Irvin, MS,§ Miguel Chaput, MD,*‡ Emmanuel Messas, MD, PhD,‡# Albert A. Hagège, MD, PhD,‡# Alain Carpentier, MD, PhD,‡# Robert A. Levine, MD,*‡# for the Leducq Transatlantic Mitral Network

ABSTRACT

BACKGROUND In patients with myocardial infarction (MI), leaflet tethering by displaced papillary muscles induces mitral regurgitation (MR), which doubles mortality. Mitral valves (MVs) are larger in such patients but fibrosis sets in counterproductively. The investigators previously reported that experimental tethering alone increases mitral valve area in association with endothelial-to-mesenchymal transition.

OBJECTIVES The aim of this study was to explore the clinically relevant situation of tethering and MI, testing the hypothesis that ischemic milieu modifies mitral valve adaptation.

METHODS Twenty-three adult sheep were examined. Under cardiopulmonary bypass, the papillary muscle tips in 6 sheep were retracted apically to replicate tethering, short of producing MR (tethered alone). Papillary muscle retraction was combined with apical MI created by coronary ligation in another 6 sheep (tethered plus MI), and left ventricular remodeling was limited by external constraint in 5 additional sheep (left ventricular constraint). Six sham-operated sheep were control subjects. Diastolic mitral valve surface area was quantified by 3-dimensional echocardiography at baseline and after 58 ± 5 days, followed by histopathology and flow cytometry of excised leaflets.

RESULTS Tethered plus MI leaflets were markedly thicker than tethered-alone valves and sham control subjects. Leaflet area also increased significantly. Endothelial-to-mesenchymal transition, detected as α-smooth muscle actin-positive endothelial cells, significantly exceeded that in tethered-alone and control valves. Transforming growth factor-β, matrix metalloproteinase expression, and cellular proliferation were markedly increased. Uniquely, tethering plus MI showed endothelial activation with vascular adhesion molecule expression, neovascularization, and cells positive for CD45, considered a hematopoietic cell marker. Tethered plus MI findings were comparable with external ventricular constraint.

CONCLUSIONS MI altered leaflet adaptation, including a profibrotic increase in valvular cell activation, CD45-positive cells, and matrix turnover. Understanding cellular and molecular mechanisms underlying leaflet adaptation and fibrosis could yield new therapeutic opportunities for reducing ischemic MR. (J Am Coll Cardiol 2016;67:275–87)

From the *Cardiac Ultrasound Laboratory, Massachusetts General Hospital, Harvard Medical School, Boston, Massachusetts; †Surgical Cardiovascular Laboratory, Massachusetts General Hospital, Harvard Medical School, Boston, Massachusetts; ‡Leducq Transatlantic Mitral Network, Fondation Leducq, Paris, France; §Center for Excellence in Vascular Biology, Cardiovascular Medicine, Department of Medicine, Brigham and Women's Hospital and Harvard Medical School, Boston, Massachusetts; ‖Vascular Biology Program, Boston Children's Hospital and Harvard Medical School, Boston, Massachusetts; ¶Department of Surgery, Boston Children's Hospital and Harvard Medical School, Boston, Massachusetts; and the #Departments of Cardiology and Cardiovascular Surgery, Assistance Publique-Hôpitaux de Paris, Hôpital Européen Georges Pompidou, University Paris Descartes, INSERM Unit 633, Paris, France. This work was supported in part by grant 07CVD04 from Fondation Leducq (Paris, France) for the Transatlantic MITRAL Network of Excellence and by the National Heart, Lung, and Blood Institute of the National Institutes of Health under award number R01HL109506 to Drs. Levine, Aikawa, and Bischoff. The content is solely the responsibility of the authors and does not necessarily represent the official views of the National Institutes of Health. Additional support was from grant K24 HL67434 from the National Institutes of Health, an American Society of Echocardiography Career Development Award, and an Erwin-Schrödinger Stipend (FWF Austrian Science Fund). The biostatistical work was conducted with support from Harvard

Listen to this manuscript's audio summary by *JACC* Editor-in-Chief Dr. Valentin Fuster.

ABBREVIATIONS AND ACRONYMS

ECM = extracellular matrix

EMT = endothelial-to-mesenchymal transition

LV = left ventricular

MI = myocardial infarction

MMP = matrix metalloproteinase

MR = mitral regurgitation

MV = mitral valve

PM = papillary muscle

SMA = smooth muscle actin

TGF = transforming growth factor

VCAM = vascular cell adhesion molecule

A common complication of ischemic heart disease, mitral regurgitation (MR) doubles mortality and increases heart failure after myocardial infarction (MI) (1). Left ventricular (LV) remodeling causes papillary muscle (PM) displacement that tethers the mitral valve (MV) leaflets and restricts closure (**Figures 1A and 1D**) (2,3).

As the left ventricle remodels, the surface area of the stretched MV increases adaptively to reduce MR (4–6). Ischemic MR remains common, however, indicating inadequate leaflet compensation (4,5). Valves excised at the late heart failure stage are stiff and fibrotic (7–9), further impairing closure by reducing systolic leaflet expansion and the flexibility needed to bend and seal effectively, as shown by finite-element analysis (10). Intrinsic MV changes are therefore important for the full pathogenesis of ischemic MR and its persistence following annuloplasty (11–13).

SEE PAGE 288

Valve adaptation can be affected not only by mechanical stretch but also by the ischemic milieu, with its known cytokine release (14–16), and by MR turbulence (17,18). We developed a large-animal model to vary these factors independently, following MV area noninvasively by 3-dimensional echocardiography (**Figures 1B, 1C, 1E, and 1F**) (4,5,19).

Tethering alone without infarction, induced surgically by PM traction short of producing MR, increased MV area and thickness over 2 months (19). The normally quiescent adult valve endothelium (20) showed reactivated endothelial-to-mesenchymal transition (EMT), an early developmental process (21–23).

How the tethered valve is affected by ischemia, with release of inflammatory cytokines and transforming growth factor (TGF)-β (14–16,24–27), is unknown. We therefore tested the hypothesis that MI alters adaptation of tethered MVs. A limited apical MI was used to avoid direct PM displacement by inferior MI (**Figure 1D**) (28). MV area changes over 2 months were explored by excised-leaflet molecular histopathology and flow cytometric analysis.

METHODS

Data from 23 adult Dorsett hybrid sheep (weight >45 kg) were compared: 6 tethered plus MI, 5 tethered plus MI with LV constraint, 6 tethered alone, and 6 sham-operated control subjects. (The last 2 groups, previously reported, now have extensive additional analyses [19]).

The tethered plus MI group required controlled leaflet tethering without MR or leaflet disruption, achieved after left thoracotomy and pericardial cradle construction under cardiopulmonary bypass. The left atrium was opened, and suture loops were inserted via the MV orifice into the exposed PM tips (both medial PM heads), buttressed by Teflon felt pledgets, and exteriorized to the epicardium overlying the PMs, pulled through a Dacron anchoring patch, in a model developed by J. Luis Guerrero. Retracting these sutures parallel to the PM axis pulled the PM tips and leaflets apically (19). The heart was restarted and a limited apical infarct produced by distal left anterior descending coronary artery ligation, avoiding directly increased PM tethering from inferior wall bulging (28). Final suture length was then adjusted in the beating heart under echocardiographic guidance just short of producing MR, the sutures were knotted against the anchoring patch, and the chest was closed.

To limit post-infarction LV remodeling and its potential effects on leaflet tethering and MV adaptation, the tethered plus MI with LV constraint group required suturing a flexible Prolene surgical mesh (Ethicon, Somerville, New Jersey) circumferentially from base to apex around both ventricles after the creation of the same MV tethering and MI model (3). This allowed us to explore MV adaptation in an ischemic milieu with limited post-infarction LV dilation.

All sheep underwent cardiopulmonary bypass, with no MI created in the tethered-alone group and no surgical intervention in the control subjects after MV and PM exposure.

Animals were cared for 58 ± 5 days and euthanized after left thoracotomy with echocardiography to confirm absence of MR and reconstruct MV surface area. These studies conformed to National Institutes

Catalyst, The Harvard Clinical and Translational Science Center (National Center for Research Resources and the National Center for Advancing Translational Sciences, National Institutes of Health award UL1 TR001102), and financial contributions from Harvard University and its affiliated academic health care centers. The content is solely the responsibility of the authors and does not necessarily represent the official views of Harvard Catalyst, Harvard University, and its affiliated academic health care centers or the National Institutes of Health. The authors have reported that they have no relationships relevant to the contents of this paper to disclose. Drs. Dal-Bianco, Aikawa, and Bischoff contributed equally to this work.

Manuscript received November 3, 2014; revised manuscript received October 16, 2015, accepted October 20, 2015.

FIGURE 1 MV Tethering and MI

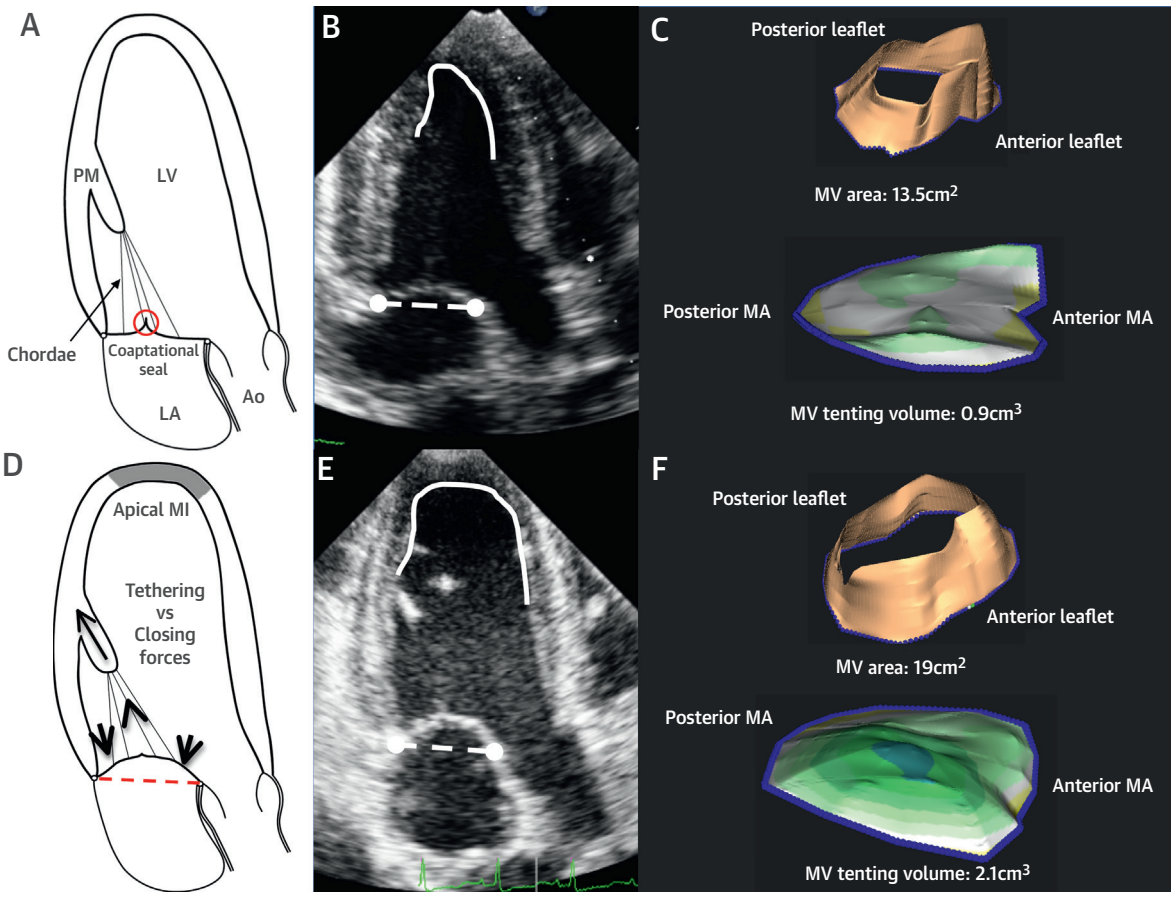

Normal mitral valve (MV) closure with convex leaflets toward the left atrium (LA) **(A)** compared with a tethered MV after papillary muscle (PM) retraction with concave leaflets **(D)**. Echocardiographic views of a sheep heart at baseline **(B)** and 2 months after PM tethering and apical myocardial infarction (MI) **(E)**. Limited apical MI results in apical left ventricular remodeling **(solid white line)** (**B** vs. **E**). Tethering of the MV leaflets relative to the annulus and tenting volume are increased (**B** vs. **E**; **C** vs. **F**, where darker colors indicate increased tenting). PM tethering and apical MI promote leaflet adaptation with increased MV surface area over time (**C** vs. **F**). Ao = aorta; LV = left ventricle; MA = mitral annulus.

of Health animal care guidelines and had institutional animal care approval.

IMAGING AND ANALYSIS. Echocardiographic data were collected using epicardial high-frequency (3.5- to 5-MHz) 2-dimensional and 3-dimensional echocardiographic probes (S5 and X3) with an iE33 scanner (Philips Medical Systems, Andover, Massachusetts). Three-dimensional volumetric datasets were ECG gated from 4 to 7 consecutive heartbeats. Full datasets were acquired in standardized planes at baseline and before euthanasia. MR absence or grading by long-axis-view vena contracta and successful MV leaflet tethering were assessed in the beating heart just after PM tethering and MI creation and again prior to euthanasia. Three-dimensional LV volumes were calculated from 6 equiangular rotated apical views. Three-dimensional tenting volume was measured between the closed leaflet atrial surface and the annular least squares plane (Figures 1C and 1F) (3).

Total MV leaflet area was measured at full diastolic opening to factor out superimposed passive systolic stretch. (Total leaflet area cannot be measured precisely in systole, because the coapted portions cannot be optimally resolved). Leaflet area was measured in a blinded fashion using validated custom Omni4D software (M. D. Handschumacher, Boston, Massachusetts) (Online Appendix) (4,29).

The left atrium was opened and the LV wall dissected from the anterolateral commissure under irrigation of pre-cooled sterile phosphate-buffered saline. Both leaflets including chordae were divided

TABLE 1 Echocardiographic Baseline and Euthanasia Measures: Tethered Plus Myocardial Infarction Model

	Baseline	Euthanasia	p Value
LVEDV, ml	57 ± 7	82 ± 17	0.023
LVESV, ml	24 ± 4	56 ± 13	0.002
LVEF, %	58 ± 3	31 ± 4	<0.001
Posteromedial PM to lateral MA trigone (systole), mm	32 ± 4	40 ± 3	<0.001
Anterolateral PM to medial MA trigone (systole), mm	29 ± 3	33 ± 2	0.010
Anterolateral to posteromedial PM distance (systole), mm	21 ± 4	26 ± 4	0.019
MV leaflet area, cm^2	13.9 ± 1.8	17.8 ± 2.3	<0.001
Leaflet length A2, mm	15.4 ± 1.8	18.6 ± 2.3	0.003
Leaflet length P2, mm	13.4 ± 1.8	16.4 ± 1.6	0.010
Annular area (diastole), cm^2	8.66 ± 1.44	11.49 ± 1.11	0.002
Annular area (systole), cm^2	7.98 ± 1.17	10.12 ± 1.28	0.006
Early systolic tenting volume, cm^3	1.76 ± 0.52	3.32 ± 0.95	0.017
Late systolic tenting volume, cm^3	0.85 ± 0.19	2.03 ± 0.69	0.009

Values are mean ± SD.

A2 = anterior mitral valve leaflet, middle scallop; LVEDV = left ventricular end-diastolic volume; LVEF = left ventricular ejection fraction; LVESV = left ventricular end-systolic volume; MA = mitral annulus; MV = mitral valve; PM = papillary muscle; P2 = posterior mitral valve leaflet, middle scallop.

for histopathology (frozen in optimal cutting temperature compound at −80°C) (Online Appendix) and cell isolation and flow cytometry (transported in pre-cooled physiological collecting medium) (Online Appendix).

Microscopy was used to measure leaflet thickness in the 10 thickest areas across the leaflet midportion and anterior and posterior strut chordal thickness.

STATISTICAL ANALYSIS. One-way analysis of variance with post-hoc contrast analysis and Tukey-Kramer test were used when appropriate to compare multiple groups of interest. Paired Student *t* tests were used to compare baseline and euthanasia results within animals. Data are summarized as mean ± SD for continuous variables and as medians with percentiles as appropriate. Statistical significance was set at $p < 0.05$ (2-sided).

TABLE 2 Echocardiographic, Histological, and Flow Cytometric Results

	Control	Tethered Alone	Tethered Plus MI	Tethered Plus MI LV Constraint
MV leaflet area increase, %	1 ± 4	17 ± 10*	28 ± 6‡	18 ± 4
MV leaflet length increase, %	0.5 ± 2.9	10.9 ± 6.8*	22.3 ± 7.5‡	10 ± 7.7
MV leaflet thickness, mm	0.42 ± 0.14	1.18 ± 0.14*†	1.61 ± 0.19	1.57 ± 0.22
VECs coexpressing α-SMA, %	7 ± 4 6 (4-11)	40 ± 19* 39 (21-59)	62 ± 16 61 (51-73)	52 ± 12 53 (44-57)
CD45-positive cells/HPF	3 ± 1 3 (2-4)	2 ± 3*† 2 (0-5)	25 ± 4 26 (22-29)	22 ± 3 20 (19-24)
Ki67-positive cells/HPF	5 ± 1 5 (4-5)	19 ± 5* 19 (15-22)	50 ± 13 51 (42-55)	35 ± 11 31 (29-45)
Microvessels/HPF	1 ± 2 0 (0-3)	1 ± 1*† 1 (0-1)	5 ± 2 5 (5-6)	4 ± 3 4 (3-6)

Values are mean ± SD or median (interquartile range). *p < 0.05, tethered only versus tethered plus MI. †p < 0.05, tethered only versus tethered plus MI LV constraint. ‡p < 0.05, tethered + MI versus tethered plus MI LV constraint.

HPF = high-powered field; LV = left ventricular; MI = myocardial infarction; MV = mitral valve; SMA = smooth muscle actin; VEC = valvular endothelial cell.

RESULTS

The tethered plus MI group sheep all had apical MI with decreased LV ejection fraction at euthanasia (from 58 ± 3% to 31 ± 4%, $p < 0.001$) and PM retraction with tented mitral leaflets (baseline vs. euthanasia, Figure 1B vs. 1E; Table 1 tenting volumes). Diastolic and systolic mitral annular area increased from baseline to euthanasia (Table 1); MR remained trace after model creation and before euthanasia (vena contracta: 0.12 ± 0.1 cm vs. 0.13 ± 0.1 cm; $p = 0.771$).

In tethered plus MI sheep, total leaflet area consistently increased by 3.9 ± 0.9 cm^2 (28 ± 6%) from 13.9 ± 1.8 cm^2 to 17.8 ± 2.3 cm^2 over 2 months ($p < 0.001$), as did leaflet length (Table 1). The leaflet area increase was greater than in animals with tethering alone or sham surgery (28 ± 6% vs. 17 ± 10% vs. 1 ± 4%, respectively, $p < 0.001$). Tethered plus MI MVs were thicker than tethered-alone MVs and 3.8 times thicker than control MVs (1.61 ± 0.19 mm vs. 1.18 ± 0.14 mm vs. 0.42 ± 14 mm, $p < 0.001$) (Table 2, Figure 2A). Increased thickness and disrupted matrix were apparent in adjacent sections stained with Masson and picrosirius red (Figures 2A and 2B). Increased leaflet size and opacity, consistent with thickening, were visible at euthanasia (Figures 2C and 2D). In the tethered plus MI sheep, although diastolic annular area increased from baseline to euthanasia by an average of 34%, there was no significant change in the ratio of leaflet to annular area as a measure of adaptation (1.61 ± 0.07 vs. 1.54 ± 0.09, $p = 0.331$), comparable with the ratio in patients with tethered versus normal leaflets (4).

CELLULAR EXPRESSION, RECRUITMENT, AND PROLIFERATION. Normal endothelial cells express CD31 but not α-smooth muscle actin (SMA) (Figure 3A). Tethering only, as previously reported, induces α-SMA expression in the endothelium on the MV's atrial side, indicating endothelial activation and EMT, with mild interstitial penetration of α-SMA-positive cells (Figure 3A) (19). In contrast, tethered plus MI sheep showed exuberant α-SMA expression along the MV's atrial side, extending deep into the interstitium (Figure 3A, right-hand panels). Expression of the endothelial cell-surface marker CD31 was diminished with tethering plus MI, further indicating EMT with loss of cell-cell contacts, allowing

FIGURE 2 Mitral Leaflet Thickness and Surface Area

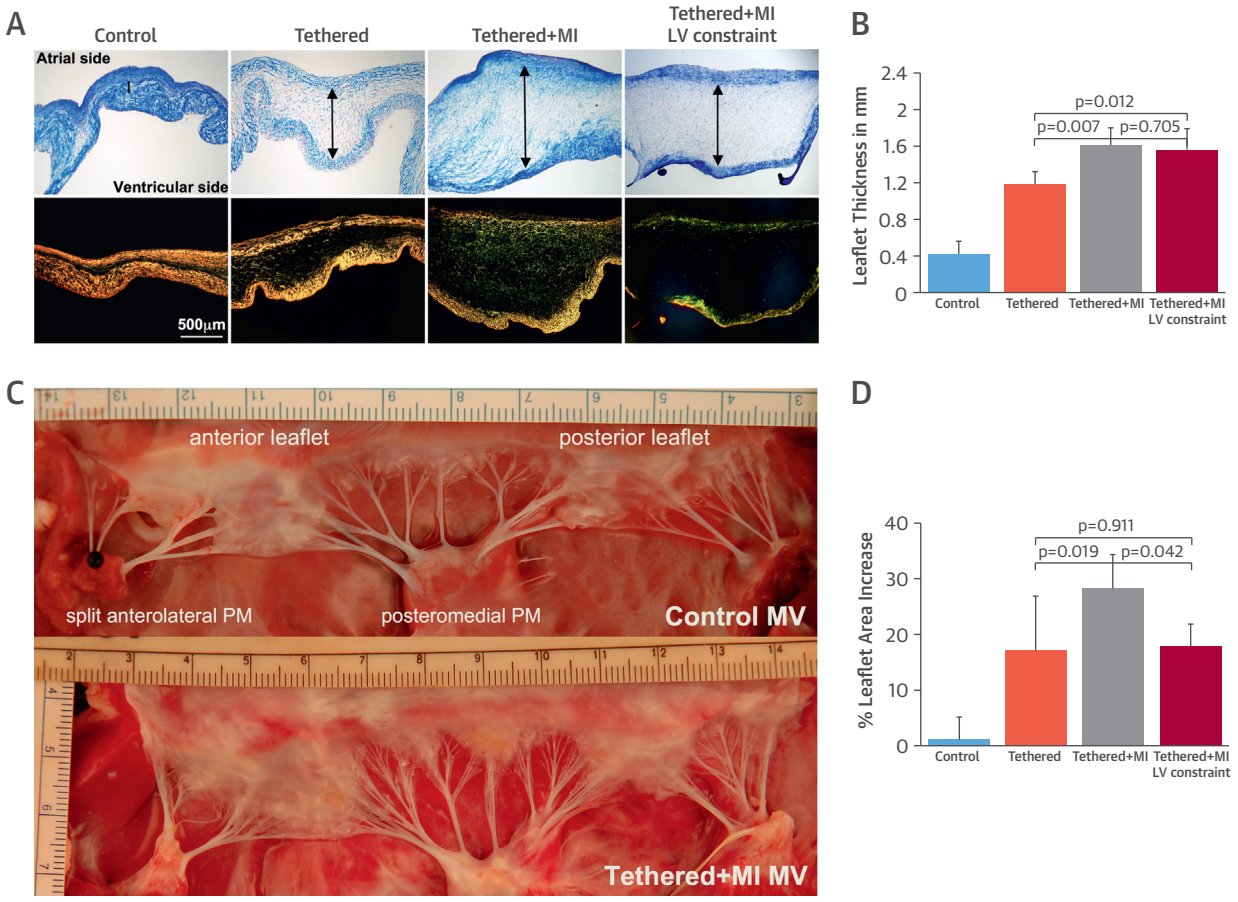

(A) Leaflet tethering alone and with myocardial infarction (MI) increases leaflet thickness via expansion of spongiosa layer **(arrows)**, even when controlled for left ventricular (LV) volume by constraint in tethered plus MI sheep (Masson, **top**; picrosirius red, **bottom**). **(B)** Quantitative comparison of leaflet thickness in all groups. **(C)** Tethered plus MI mitral valve (MV) leaflets show increased area and opacity consistent with increased thickness (centimeters). **(D)** Quantitative comparison of leaflet area increase in all groups. PM = papillary muscle.

interstitial migration (Figure 3A, third lower panel). Weak CD31 staining could be seen in isolated cells within the interstitium (Figure 3A, inset), consistent with penetration of cells undergoing EMT. Flow cytometry of cells digested from the leaflets similarly showed an increased percent of endothelial cells (CD31 positive) coexpressing α-SMA in the tethered plus MI MVs more than in tethered-alone MVs and control MVs ($62 \pm 16\%$ vs. $40 \pm 19\%$ vs. $7 \pm 4\%$, $p < 0.001$) (Figure 3B, Online Figure 1, Table 2).

Vascular cell adhesion molecule (VCAM)-1, a leukocyte adhesion molecule marking endothelial activation, was consistently expressed in the endothelium of tethered plus MI valves (Figure 4A, upper panels, and Figure 4B, red staining absent in tethered-alone MVs). TGF-β expression, not detected in normal adult valves and only mildly evident in tethered-alone MVs, was prominent on the atrial side of tethered plus MI MVs extending interstitially (Figure 4A, lower panels, and Figure 4B). Figure 4B shows adjacent sections of a tethered plus MI valve stained for α-SMA, TGF-β, collagen accumulation, and VCAM-1; all but VCAM-1 show endothelial and subendothelial colocalization.

Increased VCAM-1 along the endothelium could increase cellular recruitment into the valve. We therefore evaluated MV sections for cells expressing the hematopoietic marker CD45. Tethered plus MI MVs contained significantly more CD45-positive cells, uncommon in tethered-alone MVs and control MVs (Figures 5A and 5B). Cell proliferation detected by Ki67 immunostaining was also strongly increased in both endothelial and interstitial cells of tethered plus MI MVs (Figures 5C and 5D). CD45- and Ki67-

FIGURE 3 Mitral Valve EMT

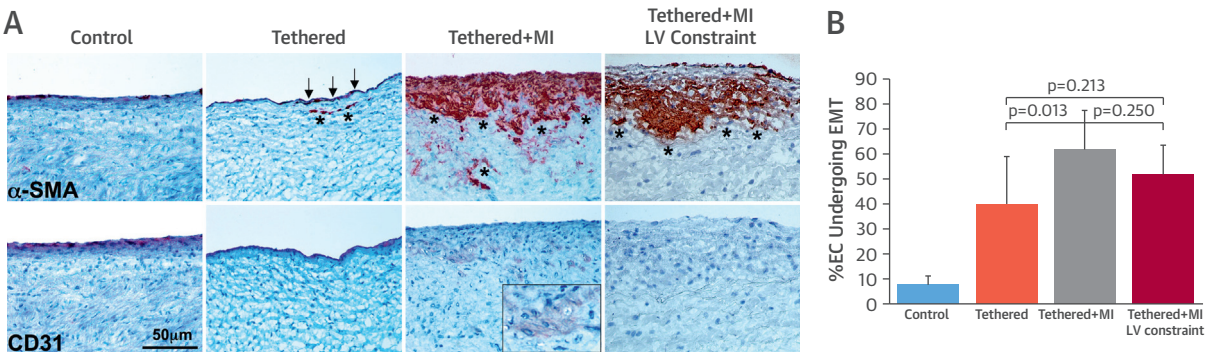

(A) Staining for interstitial marker α-smooth muscle actin (SMA) along the CD31-positive endothelium shows increasing extension of α-SMA-positive cells into the interstitium **(asterisks)** for the study groups with tethered mitral valves; occasional CD31-positive staining was seen in the interstitium. **(B)** Quantitative analysis of endothelial cells (ECs) detected by flow cytometry that are also α-SMA-positive, indicating endothelial-to-mesenchymal transformation (EMT), and expressed as percentage of total CD31-positive cells. Abbreviations as in Figure 1.

positive cells were predominantly in the atrialis and spongiosa.

INGROWTH AND REMODELING. Normal cardiac valves are largely avascular. Neovascularization is common in degenerative disease and potentially facilitates inflammation and cell recruitment. Tethered plus MI valves showed more microvessels in their midportions than tethered-alone and control MVs (Figures 5C and 5D).

Overexpression of matrix-degrading enzymes by activated myofibroblasts occurs in human myxomatous degeneration (30). The present study demonstrated abundant expression of proteolytic matrix metalloproteinase (MMP)-2 and MMP-9, particularly in the spongiosa (Figure 6), suggesting excessive collagen degradation and remodeling in tethered plus MI MVs. Picrosirius red collagen staining (Figure 2A, lower panels) confirmed these results, demonstrating poorly organized collagen in the enlarged spongiosa, also evident by Masson staining (Figure 2A, upper panels). Online Figure 2 shows heterogeneous areas of increased and reduced subatrial collagen (compare the focal collagen deposition in Figure 4B, lower left). Online Figure 3 indicates subatrial elastin loss in tethered plus MI valves.

Anterior and posterior strut chordae in the tethered plus MI sheep were thicker compared with tethered-alone and sham surgery animals (2.2 ± 1.0 mm vs. 1.2 ± 0.1 mm vs. 0.9 ± 0.1 mm, $p < 0.05$) (Figures 7A to 7C). Figures 7E and 7F show significant α-SMA expression and CD45-positive cells in tethered plus MI chordae.

LV CONSTRAINT. Three-dimensional echocardiographic analyses (Online Appendix) showed that tethered plus MI sheep had increased LV volumes and tethering distances at euthanasia compared with tethered-alone sheep. To explore whether the MV changes also occur without such increases in volume, we studied 5 additional tethered plus MI sheep in which LV volumes were limited by external constraint. With this constraint, LV volumes and tethering distances at euthanasia were comparable with those with tethering alone and significantly less than in tethered plus MI sheep without constraint (Online Appendix, Online Figure 4). Despite this reduction in LV expansion and tethering, MV changes were qualitatively and quantitatively comparable with those in tethered plus MI sheep without constraint, including consistently and prominently increased leaflet thickness (Figures 2A and 2B), EMT with extensive subendothelial α-SMA staining (Figures 3A and 3B), TGF-β and endothelial VCAM-1 staining (Figure 4A), CD45-positive cells (Figures 5A and 5B), Ki67-positive cells (Figures 5C and 5D), microvasculature ingrowth (Figures 5C and 5D), and MMP-2/MMP-9 (Figure 6). Leaflet area increased less in the constrained tethered plus MI sheep, consistent with the smaller left ventricle (Figure 2D) and potentially corresponding to the mildly but not significantly lower percentage of endothelial cells undergoing EMT and Ki67-positive cells (Figures 3B and 5D). Chordal thickness, EMT, and CD45-positive cells were also comparable (Figure 7).

DISCUSSION

This study goes beyond prior in vivo observations that mechanical MV tethering reactivates EMT, an embryonic growth process, increasing both leaflet

FIGURE 4 VCAM-1 and TGF-β Staining

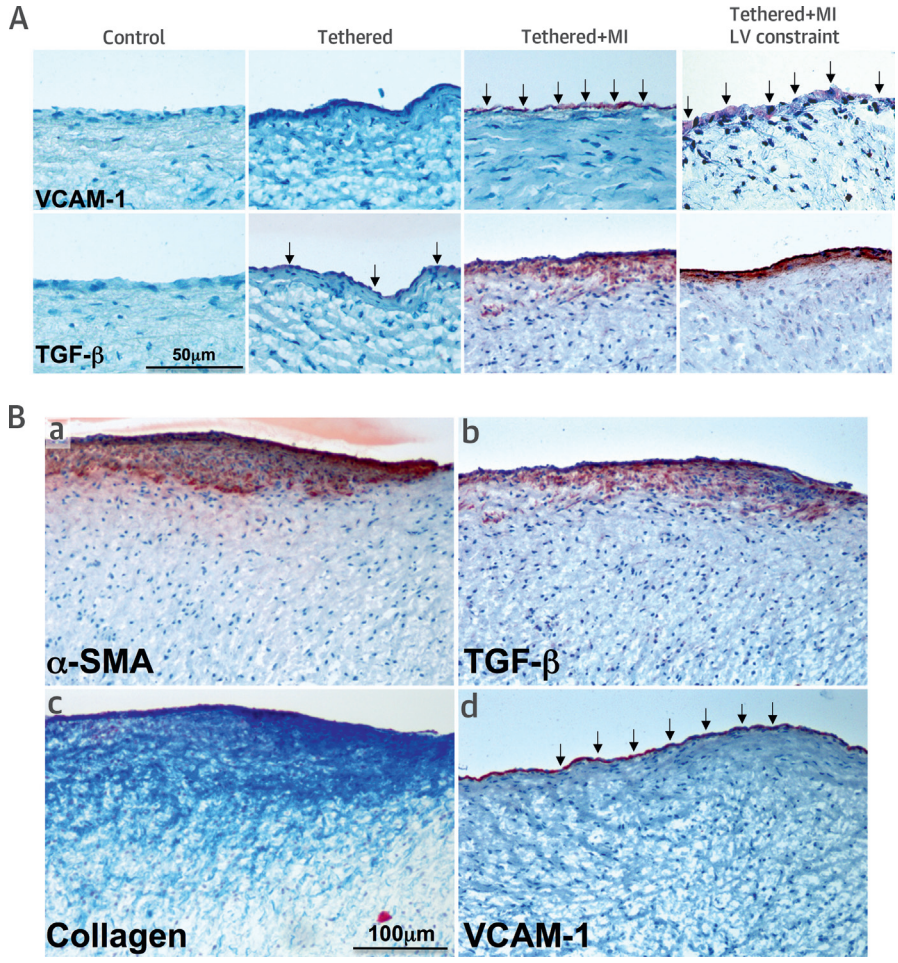

(A) Endothelial vascular cell adhesion molecule (VCAM)-1 staining (red, **upper panel**) only in the tethered plus myocardial infarction (MI) and tethered plus MI left ventricular (LV) constraint valves. Increased interstitial transforming growth factor (TGF)-β staining in tethered plus MI and tethered plus MI LV constraint valves versus tethered-alone valves **(lower panels)**. **(B)** Adjacent sections of tethered plus MI mitral valve showing colocalization of α-SMA **(a)**, TGF-β **(b)**, fibrosis (collagen accumulation) (**c**, Masson) and endothelial cell activation (VCAM-1, **arrows**, **d**).

area and thickness (19,21-23). Stretch induces valve expression of TGF-β (31), an EMT promoter (32). TGF-β was expressed but not strongly with tethering alone, suggesting that mild TGF-β induction may suffice to promote leaflet growth or that other signals may also activate EMT. These findings indicate that adult valves, normally quiescent (20), can respond to stress and altered ventricular geometry (19,20,23), as seen with their enlargement in the remodeled ventricles of patients with aortic insufficiency (33).

When apical MI is added to mechanical tethering, EMT and TGF-β are markedly augmented, with prominently increased cellular proliferation and leaflet and chordal thickness. Additional changes, previously unrecognized post-MI, occur that are not evident with tethering alone: endothelial activation, indicated by VCAM-1 expression; the presence of CD45-positive cells; neovascularization; and extracellular matrix (ECM) remodeling with increased MMP expression (**Central Illustration**).

As expected, tethering is mildly augmented by MI-induced LV remodeling, and this may contribute to changes in the MV. However, MI-induced valve changes persist when external constraint limits LV remodeling and reduces tethering distances. Furthermore, tethered-alone and tethered plus MI valves are different not only in degree of EMT,

FIGURE 5 Mitral Valve CD45-Positive Cells, Cell Proliferation, and Microvessels

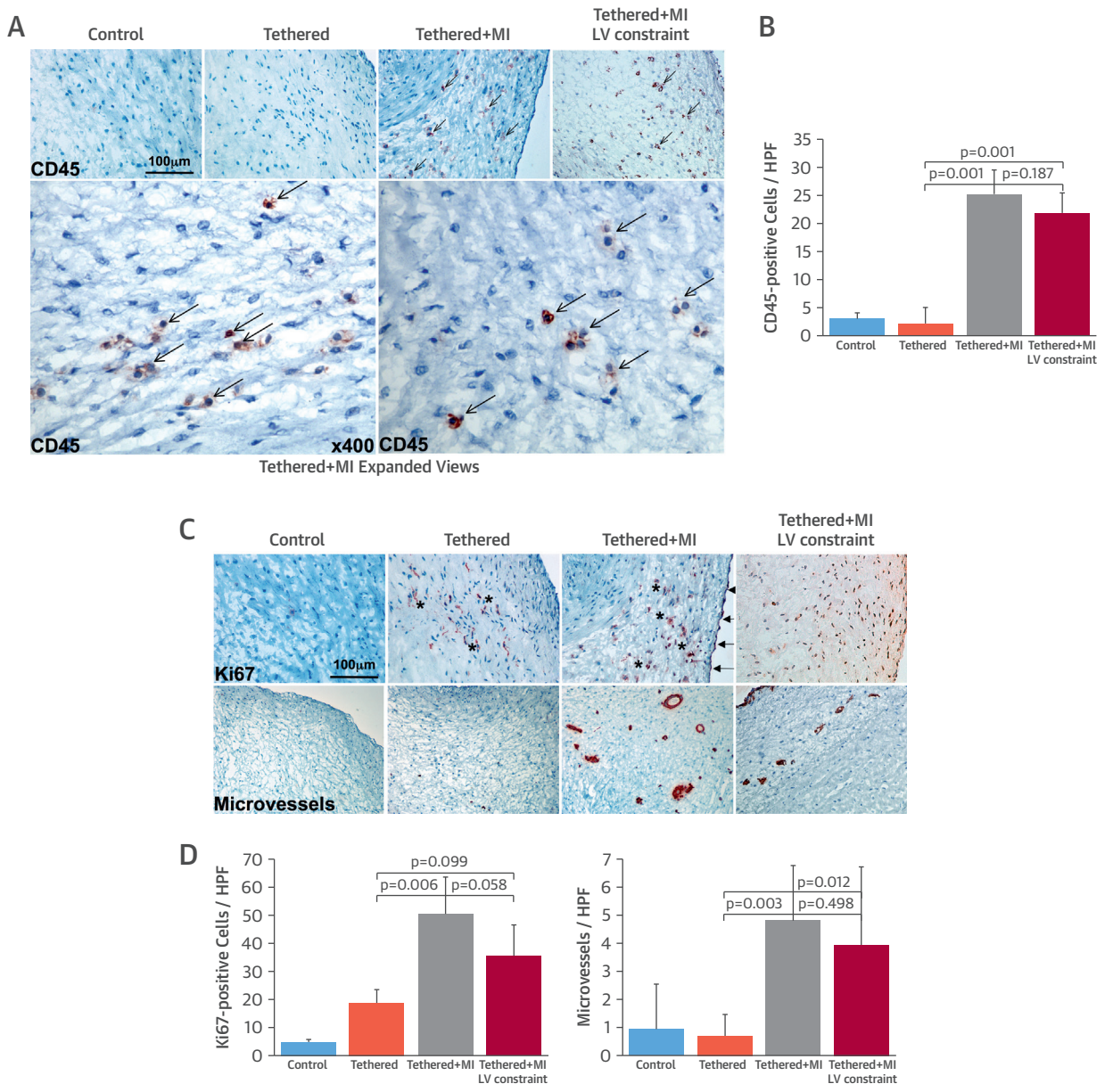

(A) CD45-positive cells **(arrows)** in tethered plus myocardial infarction (MI) and tethered plus MI left ventricular (LV) constraint valves are shown (**bottom panels**: high magnification of representative fields) and analyzed **(B)**. **(C)** Increased cellular proliferation (Ki67, **upper panels**, **asterisks**) and microvessels **(lower panels)** are greatest in tethered plus MI and tethered plus MI LV constraint valves, also seen by quantitative analysis **(D)**. HPF = high-powered field.

thickness, and TGF-β expression but also in nature of changes, with endothelial VCAM-1 activation, accumulation of CD45-positive cells, and neovascularization. The post-MI effects on MV adaptation therefore do not appear to depend solely on LV remodeling, although it seems reasonable that they may increase with LV remodeling-induced tethering.

Understanding the nature and mechanisms of post-MI MV changes can potentially provide insights into clinically important questions: Why is leaflet adaptation frequently inadequate to prevent MR post-MI, unlike adequate adaptation in aortic insufficiency (4,5,33,34)? Why does deleterious leaflet stiffening occur, impairing coaptation (8,10)? Why do current therapies have limitations (11-13)? And what

FIGURE 6 Mitral Valve Matrix MMP Staining

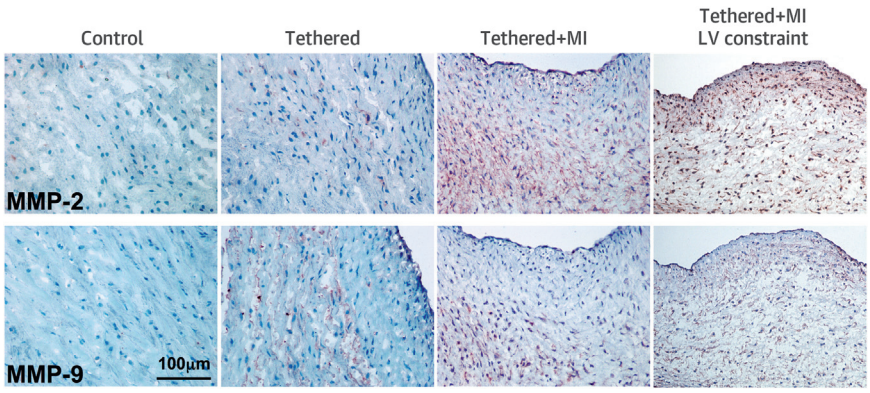

Matrix metalloproteinase (MMP-2 and MMP-9) staining is greatest in tethered plus myocardial infarction (MI) and tethered plus MI left ventricular (LV) constraint valves.

therapies might help? Several possible mechanisms influencing MV remodeling and growth active post-MI are suggested by our observations.

For example, TGF-β, profibrotic in many organs, is overexpressed in the tethered plus MI valves and seen in areas of increased collagen deposition (**Figures 4A and 4B**). Although TGF-β is a key stimulus for EMT and growth in the developing valve (21–23), it could drive valve fibrosis by activating valvular interstitial cells to become contractile α-SMA-positive myofibroblasts that secrete, compact, and remodel the extracellular matrix (24–27,35,36). The fibrogenic effects of TGF-β might be amplified by its activation of angiotensin type-1 receptors (26) that in turn would increase TGF-β expression.

TGF-β as a compensatory response to stretch may therefore become counterproductive post-MI (30), causing excessive EMT as a substrate for valve fibrosis,

FIGURE 7 Chordal Changes

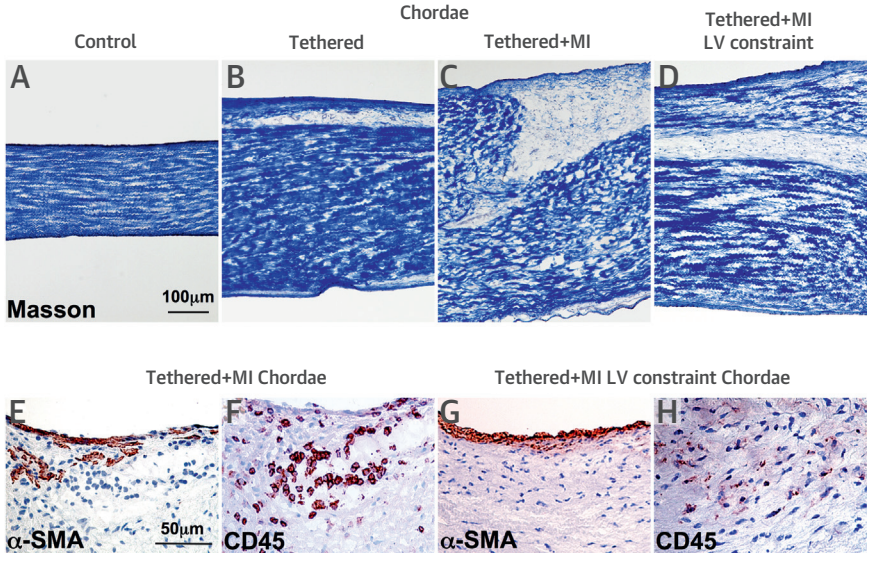

(A–D) Chordal thickness is greatest in the tethered plus myocardial infarction (MI) and tethered plus MI left ventricular (LV) constraint sheep. α-Smooth muscle actin (SMA)-positive **(E,G)** and CD45-positive **(F,H)** cells are seen near the chordal endothelium and within the interstitium in tethered plus MI and tethered plus MI LV constraint chords, suggesting chordal endothelial-to-mesenchymal transition.

CENTRAL ILLUSTRATION **Ischemia Alters Mitral Valve Adaptation: Cellular and Molecular Events in the Tethered Mitral Valve With Myocardial Infarction Compared With Tethered Valve Alone and Impact on Valve Function**

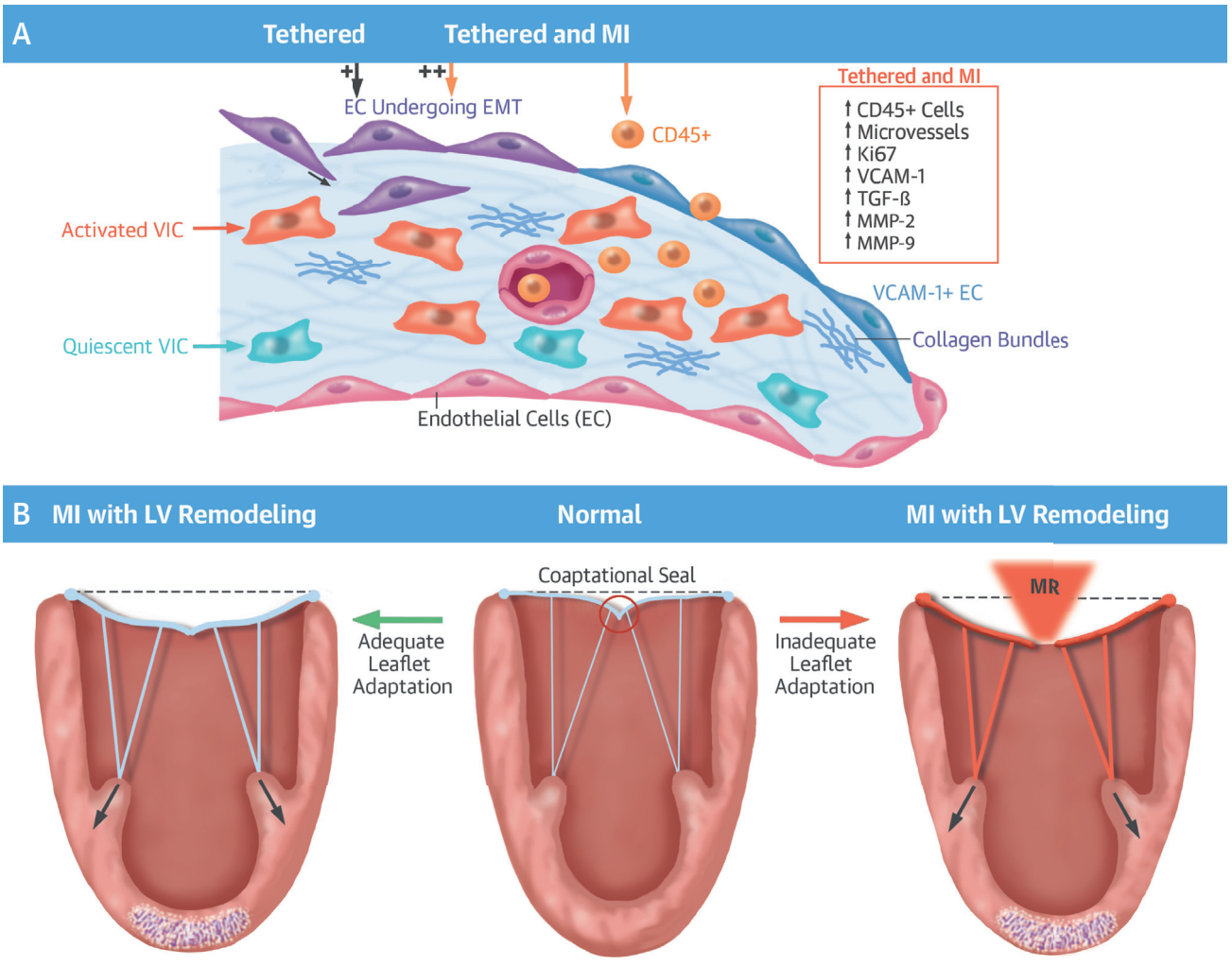

Dal-Bianco, J.P. et al. J Am Coll Cardiol. 2016; 67(3):275–87.

(A) Compared with tethered-alone leaflets, the endothelium of tethered plus myocardial infarction (MI) mitral valves (MVs) undergoes excessive endothelial-to-mesenchymal transition (EMT) and is positive for vascular cell adhesion molecule (VCAM)-1, indicating endothelial activation; the interstitium shows abundant CD45-positive cells and microvessels that may act as additional ports of cellular entry. Extracellular matrix remodeling is markedly up-regulated in tethered plus MI leaflets (increased transforming growth factor [TGF]–β and matrix metalloproteinases [MMPs]), along with a hyperproliferative increase in Ki67-positive cells. **(B)** Leaflet area increase has the potential to adapt to post-MI left ventricular (LV) remodeling and tethering and prevent mitral regurgitation (MR); inadequate area increase, with potential retraction and thickening of the tethered leaflets and chordae by induced α-smooth muscle actin–positive myofibroblasts, can augment MR following MI. EC = endothelial cells; VIC = valvular interstitial cell.

stiffening, and regurgitation (8-10,35). TGF-β may further lead to myofibroblast-induced matrix contraction (25) that can limit the ability of the valve to increase its area, possibly explaining the relative deficiency in valve area post-MI despite increased ventricular size (**Central Illustration**). TGF-β can also drive the increased chordal EMT and fibrotic thickening seen in the tethered plus MI valves (**Figure 7**), further restricting leaflet closure and increasing regurgitation.

TGF-β may originate from the stretched valve itself; TGF-β is also markedly increased in ischemic myocardium and released into the cardiac extracellular fluid (24). Conceivably, post-MI neurohumoral activation of profibrotic angiotensin II and aldosterone may promote fibrosis, synergistically with TGF-β.

Activation of the endothelial leukocyte adhesion molecule VCAM-1, seen only in the tethered plus MI valves (**Figures 4A and 4B**), suggests the presence of

inflammatory cytokines (37). Myocardial ischemia and infarction strongly induce release of proinflammatory cytokines such as tumor necrosis factor-α, interleukin-1β, and interleukin-6 from infarct zones and, later in ventricular remodeling, from noninfarcted myocardium (14–16). Endothelial activation by these cytokines recruits circulating cells into the infarct (37). Cytokines promote ECM remodeling with MMP activation, interstitial fibrosis, and collagen deposition in infarcted and remote zones (38). Infarct-induced cytokines may likewise explain the endothelial activation (VCAM-1 expression) seen in tethered plus MI valves, contributing to their matrix remodeling and abundant MMP expression (**Figure 6**).

An unexpected finding was the prominence of cells positive for CD45, considered a pan-hematopoietic cell marker, in the tethered plus MI leaflets and chordae (**Figures 5A, 5B, and 7**). Although these cells require further characterization, one hypothesis consistent with other findings is that they are fibrocytes, circulating bone marrow-derived cells that enter sites of injury and inflammation and adopt an α-SMA-positive myofibroblast phenotype (38–41). Fibrocytes, beneficial in normal wound healing and compaction, produce stiffened, sclerotic tissue in pulmonary fibrosis, asthma, and fibrosing renal and cutaneous diseases (39–41). They are also recruited to ischemic myocardium, where their inhibition reportedly reduces cardiac remodeling (42).

An equilibrium normally exists between circulating bone marrow–derived cells and the cardiac valves (43); this may be altered by activating cell adhesion molecules (37), as in the tethered plus MI valves. Marrow-derived cell recruitment is a ubiquitous response to diverse vascular and valvular injuries. Tanaka et al. (44) showed that marrow-derived cells recruited to the aortic valve display a mesenchymal phenotype in hypercholesterolemic mice.

At least a subset of the observed CD45-positive cells may therefore represent fibrocytes recruited into the stressed post-MI valve, influenced by VCAM-1 activation and TGF-β (38–40,45), which promotes their differentiation to myofibroblasts (46). Activated fibrocyte-derived myofibroblasts secrete additional TGF-β (39–41), proinflammatory cytokines, MMPs, and ECM components, reinforcing post-MI valve changes.

CLINICAL AND THERAPEUTIC IMPLICATIONS. The observations in this study suggest post-MI transition from adaptive MV enlargement to maladaptive limitation of enlargement and counterproductive stiffening (15,26). TGF-β overexpression, exuberant EMT as substrate for fibrosis, and endothelial activation with circulating cell recruitment in the fibrocyte hypothesis can promote fibrosis and matrix compaction (**Central Illustration**).

Understanding these mechanisms has potential therapeutic implications, with the long-range goal of augmenting MV area and preserving leaflet flexibility to reduce ischemic MR. TGF-β pathways can be inhibited, for example, using angiotensin type-1 receptor blockers as TGF-β antagonists to limit tissue growth in a Marfan mouse model (47). Pharmacological modification may require a specific time window to permit early EMT but prevent later fibrosis (24).

STUDY LIMITATIONS AND FUTURE DIRECTIONS. We compared changes when MI was superimposed on mechanical tethering without MR. Further work will be needed to explore the effects of MI alone, MR turbulence, and TGF-β blockade. MR alone increases MV collagen deposition, MMPs, and circulating tumor necrosis factor-α (18,48) but down-regulates myocardial noncollagen ECM components and TGF-β (49); MR combined with tethering can be tested in inferior MI. Inferior MI increases valve area, but insufficiently to prevent MR (5). Whether CD45-positive cells are beneficial or adverse needs to be explored (43,46), as do the roles of VCAM-1 and TGF-β in cell recruitment.

To determine why cellular changes (EMT, VCAM-1) mainly affect the atrial side of the MV requires testing biological differences between atrial and ventricular endothelium, compounding the higher atrialis radius of curvature and stress. Longitudinal studies are needed to explore clinically important questions of how the MV changes over time, why leaflet adaptation is frequently inadequate to prevent MR, and how this can be improved.

CONCLUSIONS

MV adaptation to mechanical stretch created by PM tethering with concomitant MI is different in nature and extent than with PM tethering alone, including exuberant EMT, cellular proliferation, TGF-β overexpression, endothelial activation, accumulation of CD45-positive cells, neovascularization, and matrix remodeling. Potential explanations based on synergistic stretch- and MI-induced pathways involve TGF-β, proinflammatory cytokines, and recruited fibrocytes. Understanding these mechanisms could lead to new therapeutic opportunities to increase leaflet area and flexibility and preserve coaptation.

REPRINT REQUESTS AND CORRESPONDENCE: Dr. Robert A. Levine, Massachusetts General Hospital, Cardiac Ultrasound Laboratory, 55 Fruit Street, Yawkey 5068, Boston, Massachusetts 02114. E-mail: rlevine@partners.org.

PERSPECTIVES

COMPETENCY IN MEDICAL KNOWLEDGE: A tethered MV has the potential for compensatory leaflet adaptation. In patients with volume overload from chronic aortic insufficiency, MV growth matches ventricular dilation, and MR is rare. With comparable ventricular dilation after MI, however, MV growth is often insufficient, and the leaflets become thick and fibrosed; MR is frequent, and heart failure and mortality risks are doubled.

TRANSLATIONAL OUTLOOK: Future research should seek to identify the cellular pathways through which post-MI tethering promotes MV leaflet and chordal growth so that therapeutic strategies can be developed on the basis of these adaptive mechanisms.

REFERENCES

1. Grigioni F, Enriquez-Sarano M, Zehr KJ, et al. Ischemic mitral regurgitation: long-term outcome and prognostic implications with quantitative Doppler assessment. Circulation 2001;103:1759–64.

2. Kono T, Sabbah HN, Rosman H, et al. Left ventricular shape is the primary determinant of functional mitral regurgitation in heart failure. J Am Coll Cardiol 1992;20:1594–8.

3. Otsuji Y, Handschumacher MD, Schwammenthal E, et al. Insights from three-dimensional echocardiography into the mechanism of functional mitral regurgitation: direct in vivo demonstration of altered leaflet tethering geometry. Circulation 1997;96:1999–2008.

4. Chaput M, Handschumacher MD, Tournoux F, et al. Mitral leaflet adaptation to ventricular remodeling: occurrence and adequacy in patients with functional mitral regurgitation. Circulation 2008;118:845–52.

5. Chaput M, Handschumacher MD, Guerrero JL, et al. Mitral leaflet adaptation to ventricular remodeling: prospective changes in a model of ischemic mitral regurgitation. Circulation 2009; 120 11 Suppl:S99–103.

6. Rausch MK, Tibayan FA, Miller DC, Kuhl E. Evidence of adaptive mitral leaflet growth. J Mech Behav Biomed Mater 2012;15:208–17.

7. Quick DW, Kunzelman KS, Kneebone JM, Cochran RP. Collagen synthesis is upregulated in mitral valves subjected to altered stress. ASAIO J 1997;43:181–6.

8. Grande-Allen KJ, Barber JE, Klatka KM, et al. Mitral valve stiffening in end-stage heart failure: evidence of an organic contribution to functional mitral regurgitation. J Thorac Cardiovasc Surg 2005;130:783–90.

9. Grande-Allen KJ, Borowski AG, Troughton RW, et al. Apparently normal mitral valves in patients with heart failure demonstrate biochemical and structural derangements: an extracellular matrix and echocardiographic study. J Am Coll Cardiol 2005;45:54–61.

10. Kunzelman KS, Quick DW, Cochran RP. Altered collagen concentration in mitral valve leaflets: biochemical and finite element analysis. Ann Thorac Surg 1998;66:S198–205.

11. Acker MA, Parides MK, Perrault LP, et al. Mitral-valve repair versus replacement for severe ischemic mitral regurgitation. N Engl J Med 2014; 370:23–32.

12. Hung J, Papakostas L, Tahta SA, et al. Mechanism of recurrent ischemic mitral regurgitation after annuloplasty: continued LV remodeling as a moving target. Circulation 2004;110:II85–90.

13. McGee EC, Gillinov AM, Blackstone EH, et al. Recurrent mitral regurgitation after annuloplasty for functional ischemic mitral regurgitation. J Thorac Cardiovasc Surg 2004;128:916–24.

14. Frangogiannis NG, Smith CW, Entman ML. The inflammatory response in myocardial infarction. Cardiovasc Res 2002;53:31–47.

15. Mann DL. Stress-activated cytokines and the heart: from adaptation to maladaptation. Annu Rev Physiol 2003;65:81–101.

16. Nian M, Lee P, Khaper N, Liu P. Inflammatory cytokines and postmyocardial infarction remodeling. Circ Res 2004;94:1543–53.

17. Fornes P, Heudes D, Fuzellier JF, et al. Correlation between clinical and histologic patterns of degenerative mitral valve insufficiency: a histomorphometric study of 130 excised segments. Cardiovasc Pathol 1999;8:81–92.

18. Stephens EH, Nguyen TC, Itoh A, et al. The effects of mitral regurgitation alone are sufficient for leaflet remodeling. Circulation 2008;118 14 Suppl:S243–9.

19. Dal-Bianco JP, Aikawa E, Bischoff J, et al. Active adaptation of the tethered mitral valve: insights into a compensatory mechanism for functional mitral regurgitation. Circulation 2009;120:334–42.

20. Aikawa E, Whittaker P, Farber M, et al. Human semilunar cardiac valve remodeling by activated cells from fetus to adult: implications for postnatal adaptation, pathology, and tissue engineering. Circulation 2006;113:1344–52.

21. Armstrong EJ, Bischoff J. Heart valve development: endothelial cell signaling and differentiation. Circ Res 2004;95:459–70.

22. Combs MD, Yutzey KE. Heart valve development: regulatory networks in development and disease. Circ Res 2009;105:408–21.

23. Markwald RR, Norris RA, Moreno-Rodriguez R, Levine RA. Developmental basis of adult cardiovascular diseases: valvular heart diseases. Ann N Y Acad Sci 2010;1188:177–83.

24. Bujak M, Frangogiannis NG. The role of TGF-beta signaling in myocardial infarction and cardiac remodeling. Cardiovasc Res 2007;74:184–95.

25. Walker GA, Masters KS, Shah DN, et al. Valvular myofibroblast activation by transforming growth factor-beta: implications for pathological extracellular matrix remodeling in heart valve disease. Circ Res 2004;95:253–60.

26. Rosenkranz S. TGF-beta1 and angiotensin networking in cardiac remodeling. Cardiovasc Res 2004;63:423–32.

27. Leask A. Potential therapeutic targets for cardiac fibrosis: TGFbeta, angiotensin, endothelin, CCN2, and PDGF, partners in fibroblast activation. Circ Res 2010;106:1675–80.

28. Gorman JH III, Gorman RC, Plappert T, et al. Infarct size and location determine development of mitral regurgitation in the sheep model. J Thorac Cardiovasc Surg 1998;115:615–22.

29. Beaudoin J, Thai WE, Wai B, et al. Assessment of mitral valve adaptation with gated cardiac computed tomography: validation with three-dimensional echocardiography and mechanistic insight to functional mitral regurgitation. Circ Cardiovasc Imaging 2013;6:784–9.

30. Rabkin E, Aikawa M, Stone JR, et al. Activated interstitial myofibroblasts express catabolic enzymes and mediate matrix remodeling in myxomatous heart valves. Circulation 2001;104: 2525–32.

31. Ku CH, Johnson PH, Batten P, et al. Collagen synthesis by mesenchymal stem cells and aortic valve interstitial cells in response to mechanical stretch. Cardiovasc Res 2006;71:548–56.

32. Person AD, Klewer SE, Runyan RB. Cell biology of cardiac cushion development. Int Rev Cytol 2005;243:287–335.

33. Beaudoin J, Handschumacher MD, Zeng X, et al. Mitral valve enlargement in chronic aortic regurgitation as a compensatory mechanism to prevent functional mitral regurgitation in the dilated left ventricle. J Am Coll Cardiol 2013;61:1809–16.

34. Saito K, Okura H, Watanabe N, et al. Influence of chronic tethering of the mitral valve on mitral leaflet size and coaptation in functional mitral regurgitation. J Am Coll Cardiol Img 2012;5:337–45.

35. Zeisberg EM, Tarnavski O, Zeisberg M, et al. Endothelial-to-mesenchymal transition contributes to cardiac fibrosis. Nat Med 2007;13:952–61.

36. Liu AC, Gotlieb AI. Transforming growth factor-beta regulates in vitro heart valve repair by activated valve interstitial cells. Am J Pathol 2008;173:1275–85.

37. Kakio T, Matsumori A, Ono K, Ito H, Matsushima K, Sasayama S. Roles and relationship of macrophages and monocyte chemotactic and activating factor/monocyte chemoattractant protein-1 in the ischemic and reperfused rat heart. Lab Invest 2000;80:1127–36.

38. Wynn TA. Cellular and molecular mechanisms of fibrosis. J Pathol 2008;214:199–210.

39. Herzog EL, Bucala R. Fibrocytes in health and disease. Exp Hematol 2010;38:548–56.

40. Keeley EC, Mehrad B, Strieter RM. Fibrocytes: bringing new insights into mechanisms of inflammation and fibrosis. Int J Biochem Cell Biol 2010;42:535–42.

41. Hong KM, Belperio JA, Keane MP, et al. Differentiation of human circulating fibrocytes as mediated by transforming growth factor-beta and peroxisome proliferator-activated receptor gamma. J Biol Chem 2007;282:22910–20.

42. Haudek SB, Xia Y, Huebener P, et al. Bone marrow-derived fibroblast precursors mediate ischemic cardiomyopathy in mice. Proc Natl Acad Sci U S A 2006;103:18284–9.

43. Visconti RP, Ebihara Y, LaRue AC, et al. An in vivo analysis of hematopoietic stem cell potential: hematopoietic origin of cardiac valve interstitial cells. Circ Res 2006;98:690–6.

44. Tanaka K, Sata M, Fukuda D, et al. Age-associated aortic stenosis in apolipoprotein E-deficient mice. J Am Coll Cardiol 2005;46:134–41.

45. Wahl SM, Hunt DA, Wakefield LM, et al. Transforming growth factor type beta induces monocyte chemotaxis and growth factor production. Proc Natl Acad Sci U S A 1987;84:5788–92.

46. Deb A, Wang SH, Skelding K, et al. Bone marrow-derived myofibroblasts are present in adult human heart valves. J Heart Valve Dis 2005;14:674–8.

47. Ng CM, Cheng A, Myers LA, et al. TGF-beta-dependent pathogenesis of mitral valve prolapse in a mouse model of Marfan syndrome. J Clin Invest 2004;114:1586–92.

48. Oral H, Sivasubramanian N, Dyke DB, et al. Myocardial proinflammatory cytokine expression and left ventricular remodeling in patients with chronic mitral regurgitation. Circulation 2003;107:831–7.

49. Zheng J, Chen Y, Pat B, et al. Microarray identifies extensive downregulation of noncollagen extracellular matrix and profibrotic growth factor genes in chronic isolated mitral regurgitation in the dog. Circulation 2009;119:2086–95.

KEY WORDS **echocardiography, endothelial-to-mesenchymal transition, inflammation, mitral regurgitation, papillary muscle**

APPENDIX **For a supplemental methods and results section as well as figures, please see the online version of this article.**